Journal of Information Display, Vol. 10, No. 3, September 2009 (ISSN 1598-0316)

Physics-based OLED Analog Behavior Modeling

Sang-Gun Lee[a] and Reiji Hattori[b]

Abstract

In this study, a physical OLED analog behavior model for SPICE simulation was described using the Verilog-A language. The model was presented through theoretical equations for the *J-V* characteristics of OLED derived according to the internal-carrier emission equation based on a diffusion model at the Schottky barrier contact, and the mobility equation based on the Pool-Frenkel model. The accuracy of this model was examined by comparing it with the results of the device simulation that was conducted.

Keywords: OLED, SPICE, physical model, theoretical equation, Verilog-A language, device simulation

1. Introduction

The driving method of active-matrix organic-light-emitting display (AMOLED) is more complex than that of liquid crystal display (LCD) because it has to be operated in an analog mode. Thus, to design these complicated circuits, precise analog circuit simulation on the pixel circuit that includes the OLED is necessary. No OLED analog behavior model has yet been developed, however, because no accurate equation representing OLED's electrical characteristics has yet been presented. Therefore, in this paper, an OLED analog behavior model that can represent OLED's electrical characteristics is proposed.

There are two types of analog behavior models: the empirical and physical models. As the former represents only the relation between the current and the voltage, the parameters that are used in such model do not have any physical meaning. On the other hand, as the physical model is based on physical equations, all the parameters used therein have a physical meaning, and the model can be applied in a wide range of temperatures and device sizes, with a simple, unique equation. The physical model is also useful for understanding the electric transport in OLED, which has not yet been made clear.

The electrical characteristics of OLED have so far been analyzed via numerical simulation, according to either the injection-limited current (J_{ILC}) or the bulk-limited current (J_{BLC}) [1, 2], but clear *J-V* equations that can represent the transition between J_{ILC} and J_{BLC} have not been provided. Therefore, in this paper, theoretical *J-V* equations representing the aforementioned transition are proposed. In the case of injection limitation, the Schottky barrier at the interface between the metal and organic layers limits the current. Generally, the current equation based on the thermionic-emission theory [3] is used, but this theory is inappropriate for organic materials since the mobility is usually too low for the theory to be applied. Therefore, in the case of organic semiconductors, which have low mobility, the injection current should follow a diffusion model [4]. On the other hand, in the case of the bulk limitation, the injected current forms a space charge, which decreases the electric field near the injection electrode in the bulk. The current-voltage characteristics are represented by the Mott-Gurney equation [5], but this equation is appropriate only when there is constant mobility. As it is well known that the mobility in organic materials usually has field dependence [6], this equation cannot be generally used. Therefore, the equations for J_{ILC} and J_{BLC} must both be updated.

This study was conducted to construct a physics-based OLED analog behavior model for SPICE simulation. The model was described using the Verilog-A language, which is the analogue expansion of Verilog-HDL and is well known for its logical description language. To construct

Manuscript Received August 31, 2009; Revised September 14, 2009; Accepted for publication September 24, 2009.
Corresponding author : Reiji Hattori
[a] Department of Information Science and Electrical Engineering, Kyushu University, 744, Nishi-ku, Fukuoka-shi, Fukuoka-Ken, Japan 802-0395
[b] Art, Science, and Technology Center for Cooperative Research, Kyushu University, 6-1 Kasuga-koen, Kasuga-shi, Fukuoka-Ken, Japan 816-8580
E-mail: hattori@astec.kyushu-u.ac.jp **Tel**: +81-92-583-7887 **Fax**: +81-92-583-7887

such analog behavior model, the theoretical *J-V* equations must be known. Device simulation can also provide the results of the *J-V* relationship, but they are not useful for SPICE simulation. In addition, the theoretical *J-V* equations are very useful for analyzing the experiment data.

The study proceeded as follows: First, the results of the OLED device simulation in a simple ETL/HTL structure, which show that some parameters have no effect on the current density-voltage (*J-V*) characteristics, were presented. The simulation was performed based on the thermionic-emission-diffusion model for the carrier injection, and on the Poole-Frenkel model for the field-dependent mobility. Next, the *J-V* characteristic equations consisting of the injection- and bulk-limited current equations were derived. Finally, a SPICE model described using the Verilog-A language was created based on the theoretical *J-V* characteristic equations. Moreover, it was confirmed that the set of *J-V* characteristics obtained from the device simulation and that of the SPICE model described using the Verilog-A language are identical.

2. OLED Device Simulation

Fig. 1 shows an energy diagram of a double-layer bipolar device, which is the simplest OLED structure. The device is composed of an electron transport layer (ETL) and a hole transport layer (HTL), and electrons and holes were injected into the ETL and HTL through the barriers ϕ_{Be} and ϕ_{Bh}, respectively. Light emission occurred in the ETL when

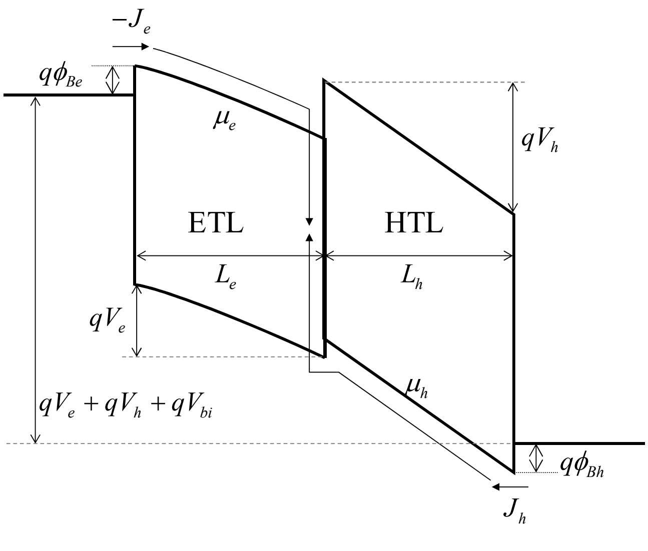

Fig. 1. Energy diagram of the double-layer bipolar device.

the internal energy barrier for the electrons was assumed to be much higher than that for the holes.

The *J-V* characteristics were simulated first by changing all the parameter values related to the electrical conduction, using the 2D device simulator ATLAS (Silvaco Co.), to evaluate how each parameter affects the *J-V* characteristics. Table 1 shows the typical parameter values that were used in the simulation, which were obtained from the literature. The simplified Poole-Frenkel mobility [7] model, which will be described later, was employed. For the sake of simplicity, the defect model related to the organic material was not considered.

The bilayered OLED has an internal heterojunction interface between the ETL and the HTL. First, the energy-band offset for the holes (ϕ_{hI}) was varied for the simulation by changing the energy-band gap of the ETL. Fig. 2 shows the *J-V* characteristics of the different ϕ_{hI}, varied from 0.1 eV to 0.5 eV. The internal energy-band offset for the electrons (ϕ_{eI}) was fixed at a sufficiently high value (0.9 eV) to prevent the injection of electrons into the HTL. It was found that the change in ϕ_{hI} has minimal influence on the J-V characteristics, as can be seen in Fig. 2. The reason for this is that more holes are accumulated in the HTL, near the interface, with an increase in ϕ_{hI}, keeping the same height from the quasi-Fermi level of the HTL to the HOMO (highest occupied molecular orbital) level of the ETL, which results in the same emission rate of the hole through ϕ_{hI}. Consequently, the value of ϕ_{hI} does not need to be considered in the theoretical *J-V* equation, but it is regarded as an important parameter in terms of the device lifetime and the transient characteristics.

Fig. 3 shows the current density dependence on the electron barrier height at cathode ϕ_{Be} for the different hole

Table 1. Material Parameters Used for the Device Simulation

Parameters	ETL	HTL	Units
Barrier height (ϕ_B)	0.1~0.5	0.1~0.5	eV
Band gap (E_g)	2.6	3.2	eV
Electric affinity (χ)	3.1	2.2	eV
Prefactor mobility (μ_0)	5 E-06	5 E-06	$cm^2V^{-1}s^{-1}$
PF activation energy (ε_a)	0.48	0.48	eV
PF factor (β)	3.7E-04	3.7E-04	$V^{-1/2}cm^{-1/2}$
BL factor (γ)	0	0	$V^{-1/2}cm^{-1/2}$
Relative permittivity (ε)	3.1	3.1	
Effective DOS (N_C)	2.50E+19	2.50E+19	cm^{-3}
Thickness (L)	50	50	nm

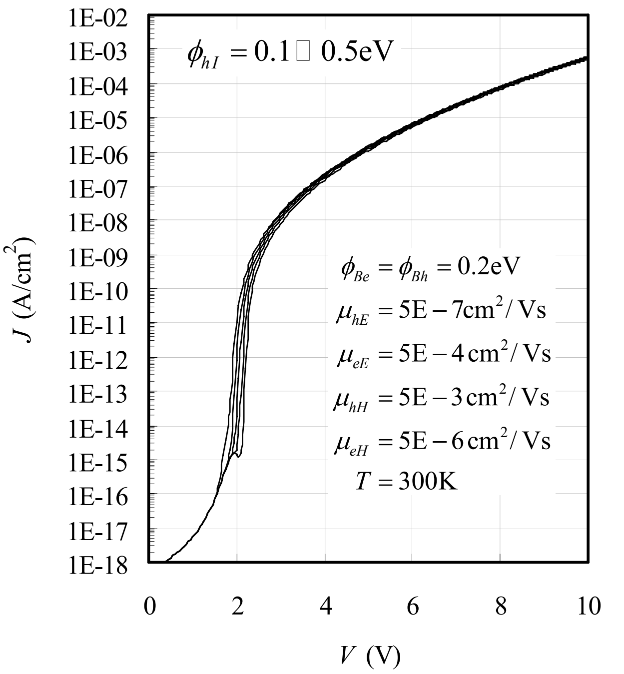

Fig. 2. *J-V* characteristics of the different internal energy-band offsets for the holes (ϕ_{hI}).

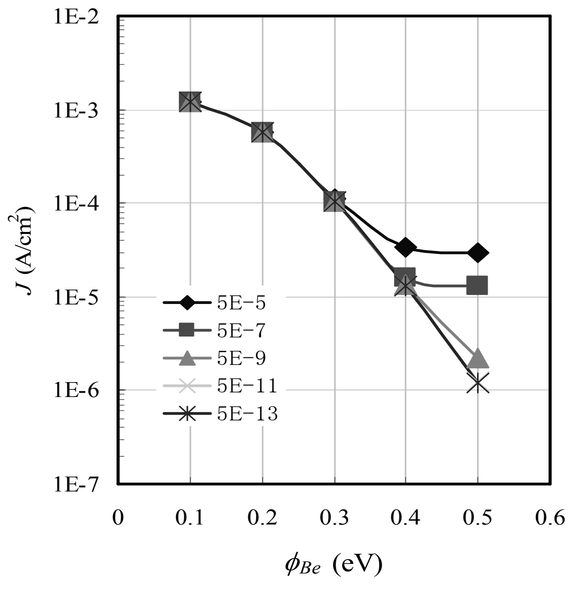

Fig. 3. J-ϕ_{Be} characteristics of the different hole mobilities in the ETL at 10 V.

mobilities (μ_{hE}) in the ETL at a 10 V applied voltage. It was found that the current density is almost independent of μ_{hE} and is influenced only when ϕ_{Be} is higher than 0.4 eV and when μ_{hE} is larger than 5E-7 $cm^2s^{-1}V^{-1}$. The current density has a constant ϕ_{Be} value under these conditions because few electrons are injected into the ETL, and when no electrons are present in the LUMO (lowest unoccupied molecular orbital) level, the holes cannot recombine with the electrons in the ETL and will thus directly reach a cathode. In this situation, the carrier balance is not kept, and the OLED device behaves like a hole-only device. These conditions are an extremely spatial case, however, and such conditions usually do not exist in OLED.

It was also confirmed that the electron mobility in the HTL (μ_{eH}) does not affect the *J-V* characteristics, which was evident in the simulation that was performed under the condition where no electrons were injected into the HTL.

3. Derivation of the Theoretical J-V Equations

3.1 Injection-limited Current (J_{ILC})

The thermionic-emission model has generally been used to represent the injection current from a metal to an organic material through the Schottky barrier. The concept is appropriate in inorganic semiconductors, which have high mobility and a long mean-free path. In the case of organic semiconductors, however, which have low mobility and a short mean-free path, the carrier injection should follow a diffusion model. Therefore, the following equation should be used to represent the injection current from a metal to an organic material:

$$J_{ILC} = q\mu EN \exp\left(-\frac{q\phi_B}{kT}\right)\exp\left(\frac{q\gamma}{kT}\sqrt{E}\right), \tag{1}$$

where q is an elemental charge, μ the mobility, E the electric field, N the density state, and ϕ_B the injection barrier height. The barrier lowering due to the image force is expressed by the last term, with the factor γ [8].

The mobility in OLED usually has field dependence. Assuming the Coulomb potential of a charged trap, the mobility is expressed by the Poole-Frenkel model, as follows:

$$\mu_{PF} = \mu_0 \exp\left(-\frac{q\varepsilon_a}{kT}\right)\exp\left(\frac{q\beta}{kT}\sqrt{E}\right), \tag{2}$$

where μ_0 is the temperature-independent prefactor mobility, ε_a the thermal-activation energy of the trapped carrier, and β the Poole-Frenkel factor as a fitting parameter. By substituting this into eq. (1) and assuming E=V/L over the whole layer, the following equations can be obtained:

$$J_{ILCe} = q\mu_{0e}N_e \frac{V_e}{L_e}\exp\left[-\frac{q(\varepsilon_{ae}+\phi_{Be})}{kT}+\frac{q(\gamma_e+\beta_e)}{kT}\sqrt{\frac{V_e}{L_e}}\right], \text{ and} \quad (3)$$

$$J_{ILCh} = q\mu_{0h}N_h \frac{V_h}{L_h}\exp\left[-\frac{q(\varepsilon_{ah}+\phi_{Bh})}{kT}+\frac{q(\gamma_h+\beta_h)}{kT}\sqrt{\frac{V_h}{L_h}}\right]. \quad (4)$$

These are the J-V equations for the injection-limited current (J_{ILC}).

3.2 Bulk-limited current (J_{BLC})

Another limitation of the current may occur in the bulk. That is, the current that is limited by the space charge effect and the following equation is given by solving Poisson's equation, including the field-dependent mobility, as shown in eq. (2) [9, 10].

$$\frac{J_{BLC}}{\mu_0\varepsilon_r\varepsilon_0}x = \frac{2}{\beta^4}\exp\left(\beta\sqrt{E}\right)\left(\beta^3E^{3/2}-3\beta^2E+6\beta\sqrt{E}-6\right), \quad (5)$$

where ε_r is the relative permittivity and ε_0 the vacuum permittivity, and where the initial field is assumed to be zero. This assumption is valid when the injection barrier is sufficiently low, or when the contact is thought to be Ohmic. In this equation, the field is a function of x and cannot be represented by V/L. To obtain the J-V relation, eq. (5) must again be integrated with x, but this will make the equation too complicated. Therefore, under the $\beta\sqrt{E} >> 1$ condition, the approximate expression can be obtained by neglecting the lower-order terms, as follows:

$$J_{BLCe} \approx \frac{2\mu_{0e}\varepsilon_{re}\varepsilon_{0e}}{\beta_e}\alpha_e^{3/2}\frac{V_e^{3/2}}{L_e^{5/2}}\exp\left(\beta_e\sqrt{\alpha_e\frac{V_e}{L_e}}\right), \text{ and} \quad (6)$$

$$J_{BLCh} \approx \frac{2\mu_{0h}\varepsilon_{rh}\varepsilon_{0h}}{\beta_h}\alpha_h^{3/2}\frac{V_h^{3/2}}{L_h^{5/2}}\exp\left(\beta_h\sqrt{\alpha_h\frac{V_h}{L_h}}\right), \quad (7)$$

where the field is assumed to be $\alpha(V/L)$ at x=L, and α is a parameter that must be adjusted to fit E to the real value.

These are the J-V equations for the bulk-limited current (J_{BLC}) with field-dependent mobility.

3.3 Transition between J_{ILC} and J_{BLC}

J-V equations (3), (4), (6), and (7) were obtained, which are valid in the different ends of the conditions where J_{ILC} and J_{BLC} are dominant, respectively. The J-V characteristics of OLED, however, must be considered J_{ILC} and J_{BLC} simultaneously. The simplest way to do this is to form an equation for the total current density, as follows:

$$J_e = \frac{J_{ILCe}\cdot J_{BLCe}}{J_{ILCe}+J_{BLCe}}, \text{ and} \quad (8)$$

$$J_h = \frac{J_{ILCh}\cdot J_{BLCh}}{J_{ILCh}+J_{BLCh}}, \quad (9)$$

where J_e and J_h are limited by the smaller current, J_{ILC} or J_{BLC}. These equations are not derived from an accurate analysis, but the transition between J_{ILC} and J_{BLC} can be well expressed.

4. Comparison of Device Simulation and Analog Circuit Simulation

The device simulation results revealed the important fact that the electron mobility in HTL (μ_{eH}), the hole mobility in ETL (μ_{hE}), and the internal energy-band offset for the holes (ϕ_{hI}) exert no influence on the J-V characteristics under ordinary conditions. Consequently, these three parameters can be eliminated in the theoretical J-V equations.

Based on the aforementioned fact, the carrier balance can be achieved in the device because the electrons are stopped by the internal barrier, all the holes recombine immediately near the interface in the ETL, and no hole can reach the cathode, except when the electron mobility in the ETL is extremely low. When the carrier balance is achieved, the following equation can be obtained:

$$J_e = J_h = J, \quad (10)$$

where J_e and J_h are the current densities of the electrons in the ETL and of the holes in the HTL, respectively, and J the total current density. Since the holes injected into the ETL immediately recombine within a narrow range near the interface under ordinal conditions, the space charge formed by the holes exerts a minimal effect on the electric-field distribution. Therefore, each layer can be treated as a single-layer device, and its J-V characteristics are given by eq. (8) and (9). As a result, the J-V characteristics are obtained by considering the double-layer device as two single-layer devices connected in series.

The voltages to be applied to each layer are given by the following equation:

$$V = V_e + V_{bi} + V_h \,, \qquad (11)$$

where V_{bi} is a built-in potential corresponding to the difference between the work functions of anode and cathode metals, V an applied voltage, and V_e and V_h the voltages applied on the ETL and HTL, respectively. When solving eq. (10) and (11) for the ETL and HTL simultaneously, J is decided uniquely by V, but the equations cannot be solved in an algebraic manner.

To solve eq. (1)-(11) simultaneously, the equivalent circuit shown in Fig. 4 was used. The built-in voltage (V_{bi}) is expressed by the voltage source. Once the equation representing the relationship between the output and the input are obtained, it is easy to generate the analog behavior model using the Verilog-A language. The Verilog-A language is the computer programming language and an analogue expansion of Verilog-HDL. In addition, since the Verilog-A language can treat an internal node, its use makes it possible to solve the equations simultaneously, although not in an algebraic manner. The *J-V* characteristics of the model described using the Verilog-A language are shown in Fig. 5. The fields in each layer, E_E and E_H, are given by dividing the voltages applied on each diode by each layer thickness. Eq. (10) is automatically satisfied by connecting the diodes in series.

Fig. 5 shows the results of the *J-V* characteristics from the analog circuit simulation, using the Verilog-A language as a parameter of the Schottky barrier height for the hole at the anode, and compares these with the results of the *J-V* characteristics from the device simulation. The barrier height for the electron at the cathode (ϕ_{Be}) was fixed at 0.2 eV. In both calculations, the same physical model and parameters were employed. As shown in Fig. 5, the device simulation and analog circuit simulation results were in agreement, expect for those cases where there was a low voltage range. The *J-V* curves increased when the barrier height decreased, and the increase was discontinued at less than 0.2 eV due to J_{BLC}.

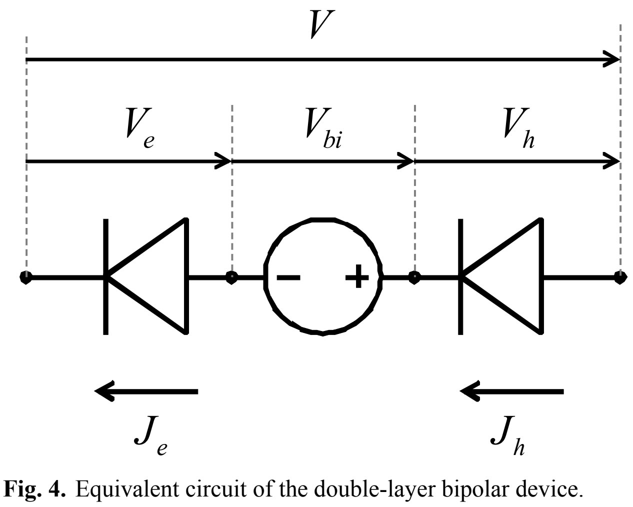

Fig. 4. Equivalent circuit of the double-layer bipolar device.

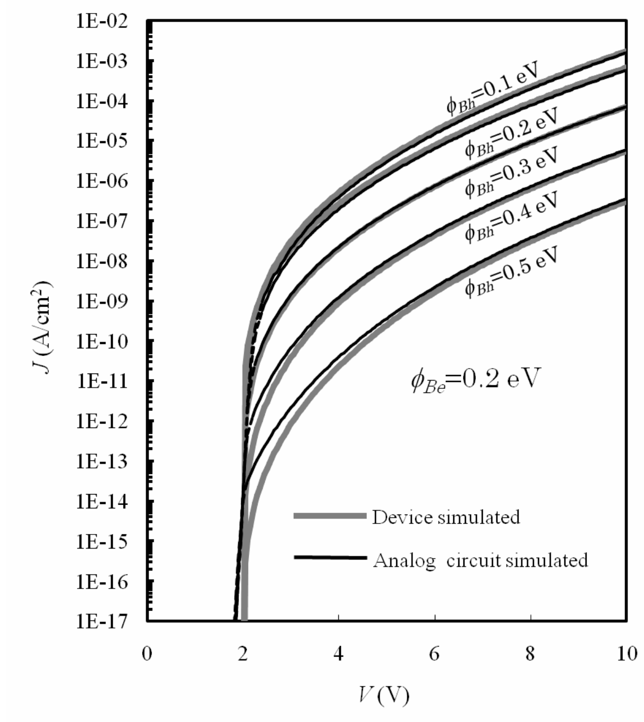

Fig. 5. Comparison of the *J-V* characteristics of the double-layer OLED in the results of the device and analog circuit simulations.

5. Conclusions

Theoretical *J-V* equations in double-layer bipolar devices were successfully derived in this study. These theoretical equations include all the parameters related to the electric transport but exclude the parameters of the electron mobility in the HTL, the hole mobility in the ETL, and the internal energy-band offset for the holes because they do not exert any influence on the *J-V* characteristics. Moreover, these equations can represent the transition between the injection-limited current and the bulk-limited current. Using these equations, an analog circuit simulator was described with the SPICE model using the Verilog-A language, showing a good agreement with the results that were obtained from the device simulation.

References

[1] G. G. Malliaras and J. C. Scott, *J. Appl. Phys*. **85**, 7426 (1999).

[2] P. S. Davids, I. H. Campbell, and D. L. Smith, *J. Appl. Phys*. **82**, 6319 (1997).

[3] V. I. Arkhipov, E. V. Emelianova, Y. H. Tak, and H. Bässler, *J. Appl. Phys*. **84**, 848 (1998).

[4] S. M. Sze, Physics of Semiconductor Device (Wiley-Interscience, New York, 2nd edition, 1981), p. 254.

[5] K. C. Kao, and W. Hwang, Electrical transport in solids (Pergamon Press, Oxford, 1981), p. 145.

[6] J. G. Simmons, *Phys. Rev*. 155, 657 (1967).

[7] J. Frenkel, *Phys. Rev*. **54** ,647 (1938).

[8] W. D. Gill, *J. Appl. Phys*. **43**, 5033 (1972).

[9] P. N. Murgatroyd and H. H. Wills, *J. PHYS.D: Appl. Phys*. **3**, 151 (1970).

[10] D. F. Barba, J. PHYS.D: *Appl. Phys*. **4**, 1812 (1971).